Articular chondrocyte-derived exosomes promote cartilage differentiation of human umbilical cord mesenchymal stem cells by activation of autophagy

Ke Ma (gxykmk@163.com)
Guangxi Medical University https://orcid.org/0000-0003-1321-3032
Bo Zhu
Guangxi Medical University
Zetao Wang
Guangxi Medical University
Peian Cai
Guangxi Medical University
Mingwei He
Guangxi Medical University
Danyan Ye
Second Affiliated Hospital of Shantou University Medical College
Guohua Yan
Guangxi Medical University
Li Zheng
Guangxi Medical University
Lujun Yang
Second Affiliated Hospital of Shantou University Medical College
Jinmin Zhao
Guangxi Medical University

Research

Keywords: autophagy, chondrocytes, chondrogenesis, exosomes, human umbilical cord mesenchymal stem cells

Posted Date: August 11th, 2020

DOI: https://doi.org/10.21203/rs.3.rs-23463/v2

Version of Record: A version of this preprint was published on November 9th, 2020. See the published version at https://doi.org/10.1186/s12951-020-00708-0.

Abstract

Background Umbilical cord mesenchymal stem cell (HUCMSC)-based therapies were previously utilised for cartilage regeneration because of the chondrogenic potential of MSCs. However, chondrogenic differentiation of HUMSCs is limited by the administration of growth factors like TGF-β that may cause cartilage hypertrophy. It has been reported that exosomes could modulate the phenotypic expression of stem cells. However, the role of human chondrogenic-derived exosomes (C-EXOs) in chondrogenic differentiation of HUCMSCs has not been reported. Results In this study, we successfully isolated chondrocyte-derived exosomes (C-EXO) from human multi-finger cartilage and found that C-EXO efficiently promoted the proliferation and chondrogenic differentiation of HUCMSCs, evidenced by highly expressed aggrecan (ACAN), COL2A and SOX-9. Also, the expression of the fibrotic marker, COL1A and hypertrophic marker, COL10, was significantly lower than that induced by TGF-β. In vivo, stimulation of C-EXO accelerated HUCMSCs-mediated cartilage repair in rabbit models. Furthermore, C-EXO led to increasing autophagosomes during the process of chondrogenic differentiation, indicating that C-EXO promoted cartilage regeneration might be through the activation of autophagy. Conclusions C-EXOs play an essential role in fostering chondrogenic differentiation and proliferation of HUCMSCs, which may be beneficial for articular cartilage repair.

Introduction

Regeneration of damaged articular cartilage remains a challenge for cartilage repair. In the clinic, current treatment strategies for cartilage injuries, including microfracture and autogenous cartilage transplantation, are not satisfactory. In recent years, stem cell-based strategies using multipotent mesenchymal stem cells (MSCs), which have the ability of self-renewal and can be specifically differentiated into chondrocytes,[1,2] has emerged as a promising modality for cartilage regeneration.

The chondrogenic differentiation of MSCs is profoundly affected by the extracellular microenvironment and various growth factors[3][Jayasuriya, 2016, The influence of tissue microenvironment on stem cell–based cartilage repair]. TGF-β (Transforming growth factor-beta) is recognised as the main transforming growth factor[4,5] that has the potential to induce the direct differentiation of mesenchymal stem cells to chondrocytes[6,7]. However, TGF-β also causes cartilage hypertrophy during the process of cartilage differentiation[5], and the application of TGF-β leads to complications such as functional heterogeneity, degradation, and loss of activity, which ultimately limits its clinical applications. Hence, it is imperative to find alternative small molecular substances that are functionally homogenous for cartilage regeneration.

Exosomes are a class of secreted vesicles with nano-size that have been identified as the crucial intermediate cell mediator of intercellular communication through the transfer of bioactive components, including various proteins and microRNAs, thereby affecting the phenotype and function of recipient cells[8-11]. Current studies have found that exosomes are released by multivesicular bodies (MVBs) from parental cells[12]. Therefore, exosomes reflect the composition of parental cells to a certain extent. According to its source and parental cell status, exosomes display a variety of functions such as tissue

regeneration, immune regulation, and gene regulation[13-15]. In recent years, the role of exosomes in tumours and immunology has been extensively studied. However, the role of exosomes as an inducer of stem cell differentiation has rarely been studied. An *in vitro* study showed that exosomes derived from osteoblasts could promote stem cell differentiation into osteoblasts, while exosomes derived from adipocytes induced adipogenic differentiation of stem cells in an osteogenic medium environment[16]. These findings indicate that exosomes retain the multiple biological activities of homologous cells[17]. Another study found that exosomes derived from rabbit chondrocytes can promote the formation of ectopic cartilage in the subcutaneous environment of cartilage progenitor cells[18], suggesting that chondrocyte-derived exosomes play a crucial role in chondrogenesis of cartilage progenitor cells. Thus, human articular chondrocytes-derived exosomes (C-EXOs) may be promising substitutes for TGF-β to guide chondrogenic differentiation of MSCs. However, this strategy has not been studied yet.

Among various types of MSCs, human umbilical cord mesenchymal stem cells (HUCMSCs), which are derived from Wharton's jelly, the primitive connective tissue surrounding umbilical cord vessels, are attracting increasing attention because they exhibit unique properties of higher proliferation rates, immunosuppression, and lower immunogenicity, as well as relatively easy and non-invasive isolation procedures compared to other sources of derived MSCs [19-21]. Therefore, HUCMSCs are the ideal and noncontroversial cell source for regenerative medicine and hold promise in cartilage regeneration and repair.

In this study, we demonstrated that human C-EXOs could promote the proliferation and chondrogenic differentiation of HUCMSCs, which are beneficial to cartilage regeneration *in vivo*. Chondrogenic differentiation by C-EXOs may be associated with the activation of autophagy in HUCMSCs. This study may provide a reference for the clinical application of exosomes in cartilage repair.

Results

Characterisation of HUCMSCs

To examine the morphology of HUCMSCs isolated from human umbilical cord tissue, HUCMSCs at passage 3-5 were observed using optical microscopy. As shown in Fig. 1A, HUCMSCs exhibited a fibroblastic and spindle-shaped morphology, which are typical morphological characteristics of MSCs. Moreover, the multipotency of isolated HUCMSCs was also evaluated by different inductive conditions. The osteogenic, adipogenic, and chondrogenic differentiation of HUCMSCs was verified using alizarin red staining, oil-Red-O staining, and alcian blue staining, respectively. A high degree of mineralisation, intracytoplasmic lipid droplet accumulation, and positive chondrogenic mucopolysaccharide staining were observed in each corresponding staining (Fig. 1B-D). Additionally, HUCMSC-specific markers were detected using flow cytometry. HUCMSCs were positive for the typical stem cell surface markers CD29, CD105, and CD44, but were negative for the hematopoietic lineage markers CD34 and CD45 (Fig. 1E&F).

Characterisation of human articular chondrocyte-derived exosomes (C-EXOs)

To obtain articular chondrocyte-derived exosomes, we first isolated and cultured human articular chondrocytes, which exhibited their cobblestone-like morphology (Fig. 2A). Exosomes were isolated from the conditioned medium of chondrocytes. Transmission electron microscopy (TEM) showed the spheroid morphology of the exosomes purified from chondrocytes (Fig. 2B). To check the particle size of the exosomes, we performed Flow Nano Analysis (NanoFCM) and confirmed that the size was within 40-150 nm in diameter (Fig. 2C). The exosome-related markers CD9 and CD63 were detected using NanoFCM (Fig. 2D). Further, the levels of CD63, CD9, TSG101, and CALNEXIN in C-EXOs and chondrocytes were analysed by western blotting. As shown in Figure 2E, CD63, CD9 and TSG101 proteins were expressed in C-EXO, but not CALNEXIN. Collectively, these results indicate that exosomes derived from human articular chondrocytes were successfully isolated and identified. Moreover, to investigate the feasibility of using C-EXOs for the treatment of cartilage defects, we examined cellular uptake of C-EXOs by HUCMSCs *in vitro*. After incubation of HUCMSCs with FITC-labelled C-EXOs for 12 hours, fluorescence microscopy images revealed that FITC-labelled C-EXOs were present in the cytoplasm of HUCMSCs, confirming that C-EXOs were internalised successfully by HUCMSCs (Fig. 2F).

C-EXOs accelerate the proliferation and migration of HUCMSCs

To assess the effect of C-EXOs on the proliferation of HUCMSCs, we detected the viability of HUCMSCs cultured with various doses of C-EXOs. According to the result of CCK8 analysis, C-EXOs promoted HUCMSC growth in a dose-dependent manner. Among the concentrations, the corresponding productivity of HUCMSCs appeared at the highest level at 9×10^7 particles per mL (Fig. 3A). Thus, this concentration was selected and used as the added concentration for the following experiments. The results of both the live/dead cells viability assay and flow cytometry analysis showed that the proportion of live cells/dead cells in the C-EXO group was comparable with the control group. However, the proportion of apoptotic cells was higher in the TGF-β group compared with the C-EXO group, indicating that C-EXO stimulation did not lead to HUCMSC apoptosis *in vitro* (Fig. 3B-D). To analyse whether the migratory ability of HUCMSCs was affected by C-EXOs, HUCMSCs were incubated with C-EXOs for 6 and 12 hours. The results of the Scratch wound healing experiment showed that both C-EXOs and TGF-β significantly enhanced the migratory capacity of HUCMSCs relative to the control. Notably, C-EXOs exhibited a more positive effect on the motility of HUCMSCs than TGF-β did at every time point (Fig. 3E-G). These results implied that C-EXOs promote the proliferation of HUCMSCs, although the underlying mechanism needs to be clarified further.

C-EXOs promote the chondrogenic differentiation of HUCMSCs

To investigate a possible role of C-EXOs in chondrogenic differentiation, HUCMSCs were allowed to undergo chondrogenic differentiation in the absence or presence of C-EXOs. TGF-β was used as a positive control. As shown in Fig. 4A, we observed that the expression of the cartilage-specific marker Col2a was slightly downregulated during the initial period. Nevertheless, after prolonged stimulation of C-EXOs, the expression of Col2a dramatically increased at 14 and 21 days, and the expression of Sox9 and ACAN, known to be involved in chondrogenesis, was significantly increased at each time point after C-EXO treatment compared with the negative control, as demonstrated by RT-PCR analysis. The upregulation of these genes was comparable with that in the TGF-β induction group. Of note is that the expression of Col1a, a fibrocartilage marker, was also elevated at early stages, but significantly decreased at later stages (14 days and 21 days) in both the C-EXO and TGF-β group compared with controls. In addition, we also examined the expression of the hypertrophic cartilage-enriched marker Col10, and found its expression to be equal to Col1a at 3 and 7 days.

In contrast, it was heavily downregulated in the C-EXO group compared with the untreated group. Still, it maintained a relatively high level in the TGF-β group at 14 and 21 days (Fig. 4B). Western blot analysis also showed COL2A, SOX9, and ACAN protein expressions were significantly upregulated, whereas COL1A and COL10 protein expressions were downregulated in the C-EXO group. Notably, the expression of COL10 protein also remained at high levels in the TGF-β group (Fig. 4C). Measurements of glycosaminoglycans (GAG) were carried out using the established DMMB (1,9-dimethylmethylene blue) assay. The level of GAG accumulation was normalised by DNA content, which served as the cell number control. As expected, GAG production was increased in both the C-EXO and TGF-β groups; however, the timepoint at which it was increased was earlier for the C-EXO group (3 days) than the TGF-β group (Fig. 4D). Furthermore, the results of immunofluorescence staining for COL2A further demonstrated that COL2A expression was more elevated than the negative control at 21 days in both the C-EXO and TGF-β groups (Fig. 4E–F), which is consistent with the RT-PCR results. Taken together, these data strongly suggest that C-EXOs contribute to the chondrogenic differentiation of HUCMSCs, and their influence is more beneficial than TGF-β owing to the ability of C-EXOs to maintain the phenotypic stability of chondrocytes.

C-EXOs promote chondrogenesis by activating autophagy in HUCMSCs

Given that C-EXOs promoted the chondrogenic differentiation of HUCMSCs and that autophagy plays a significant role in cell differentiation[22,23], we investigated whether autophagy activation will occur during the chondrogenic differentiation of HUCMSCs mediated by C-EXOs. First, HUCMSCs were transfected with mRFP-GFP-LC3 virus and cultured with or without C-EXOs, and autophagic flux was observed using laser confocal microscopy. LC3, a key protein concentrated on autophagic precursors and autophagosome membranes, can indicate the existence of autophagy. After the cells were transfected with dual fluorescent lentivirus, if autophagy occurs, LC3 on autophagosome precursors and autophagosome membranes fluoresce. Under the excitation light of different wavelengths of confocal

microscopy, two colours were observed: mRFP red fluorescence and GFP green fluorescence, and the two types of fluorescence would combine as yellow fluorescence in the synthetic image. As shown in Fig. 5A, there were more yellow and red fluorescence dots in the C-EXO group than in the TGF-β and negative control groups (Fig. 5A&B), indicating a higher number of autophagosomes in the C-EXO-treated HUCMSCs. Moreover, the appearance of autophagosomes was confirmed in C-EXO- or TGF-β-treated HUCMSCs by transmission electron microscopy (TEM). The C-EXO group showed more autophagosomes than the other groups (Fig. 5C), which is in line with the results of laser confocal microscopy. Further western blotting results showed that in the C-EXO group, the expression levels of HUCMSC autophagy of the positively correlated proteins Beclin-1, ATG7, and LC3-B were increased. In contrast, the expression level of the negatively correlated protein P62 was decreased (Fig. 5D&E). Thus, C-EXO stimulation induced the chondrogenic differentiation of HUCMSCs by activating autophagy *in vitro.*

C-EXOs promote cartilage repair during HUCMSC-mediated cartilage regeneration *in vivo*

To further test the cartilage repair efficacy of C-EXOs, we generated an articular cartilage defect model in rabbits. None of the rabbits displayed signs of post-operative infection or lameness during the 12-week post-transplantation period. Repair of articular cartilage defects was assessed at 4 and 12 weeks after HUCMSC implantation surgery. As shown in Fig. 6A, 4 weeks after transplantation, the macroscopic appearance of all three groups displayed recognisably regenerated tissue. Interestingly, in a comparison of all groups, the regenerated tissues in the C-EXO and TGF-β groups were better than the control group, in which the hyaline-like cartilaginous repair tissue filled most of the defects in the C-EXO group. In contrast, other defects treated with TGF-β-induced HUCMSCs were partially filled with repair tissue, and the concave surface of the regenerated tissue was larger than that of the C-EXO group. After 12 weeks, there was still a noticeable hole in the tissue surface of the control group, the cartilage defect was nearly devoid of regenerative tissue, with only amorphous soft fibres observed in the central area of the defect. The repaired tissues of the treatment groups were almost identical to healthy cartilage tissue. Notably, the newly formed tissues in the C-EXO groups had a smooth white appearance and fused with the surrounding healthy cartilage; its surface topography was more similar to that of the host cartilage compared with that of the TGF-β group, whose regenerated tissue surfaces within the defect were fairly rough (Fig. 6A). Further quantitative assessment of repaired tissue showed that both the C-EXO group and the TGF-β group had significantly higher ICRS scores (mean ± SD of 16.125±1.25, mean ± SD of 15.75±1.83, respectively) than the control group (mean ± SD of 7.75±1.67) (p□0.05) (Fig. 6B). In addition, the gross morphological findings were supported by histological evidence. H&E staining showed that only a small amount of fibrous tissue was observed in the periphery of the defect and lacked hyaline-like cartilaginous tissue in the control group, suggesting limited intrinsic repair capability.

In contrast, regenerated tissues in the C-EXO and TGF-β groups presented a smooth surface like hyaline cartilage with regular cellular tissue, which was more abundant and thicker than those in the control group (Fig. 6C). Safranin O-Fast Green staining demonstrated the changes in the quantity of proteoglycan

in the cartilage matrix. As shown in Fig. 6D, the content of proteoglycan in the C-EXO group is relatively large and evenly distributed in the cartilage matrix at 12 weeks. The cartilage-like tissues entirely occupied the defects, the regenerated tissue was similar in colour and texture to native cartilage, and even the formation of the cartilage matrix was closer to healthy cartilage.

In contrast, the production of proteoglycan was lower in the TGF-β group compared with the C-EXO group. In addition, at week 12, positive expression of collagen type was found in the C-EXO group and TGF-β group, but not in the control group, and the positive expression of collagen type in the C-EXO group was more similar to healthy tissues (Fig. 6E). Quantitatively, the mean score of the control group was significantly lower than that of the C-EXO group and the TGF-β group. Among these groups, C-EXO treatment exhibited the best restorative effect (Fig. 6F). Taken together, these results suggested that C-EXOs can promote cartilage defect repair in HUCMSC-mediated cartilage regeneration.

Discussion

In this study, we demonstrated that chondrocyte-derived exosomes could promote chondrogenic differentiation of HUCMSCs by activating autophagy *in vitro* and improve the effect of HUCMSC-mediated cartilage repair *in vivo*.

During the repair of articular cartilage defects using the stem cells, the microecological environment of the tissue should have the same characteristics as the host cartilage. One of the main niche cell types in the joint is chondrocytes, which play an important role in maintaining the microenvironment in the joint cavity. In our study, we found that C-EXOs could promote the chondrogenesis of HUCMSCs and exert a therapeutic effect on cartilage defects, suggesting that the C-EXOs a pleasant micro-ecological environment for cartilage repair. This finding is consistent with previous studies that exosomes derived from mature chondrocytes can promote the formation of ectopic cartilage in the subcutaneous environment of cartilage progenitor cells[18]. Exosomes, as important paracrine components, are involved in maintaining normal physiological functions, mediating inter-cell communication, and inducing changes in cell functions and processes by delivering various types of bioactive microRNAs, proteins, and unique gene products[9,10,24]. These microRNAs might serve as vital inducers of HUCMSC differentiation into chondrocytes, such as the exosomal miR-92a-3p, exosomal miR-95-5p, exosomal miR-320c, and exosomal miR-135b, which can regulate cartilage development and homeostasis[25-28][, 2019, Expression of exosomal microRNAs during chondrogenic differentiation of human bone mesenchymal stem cells - Sun - 2019 - Journal of Cellular Biochemistry - Wiley Online Library][, 2019, Expression of exosomal microRNAs during chondrogenic differentiation of human bone mesenchymal stem cells - Sun - 2019 - Journal of Cellular Biochemistry - Wiley Online Library][, 2019, Expression of exosomal microRNAs during chondrogenic differentiation of human bone mesenchymal stem cells - Sun - 2019 - Journal of Cellular Biochemistry - Wiley Online Library][, 2019, Expression of exosomal microRNAs during chondrogenic differentiation of human bone mesenchymal stem cells - Sun - 2019 - Journal of Cellular Biochemistry - Wiley Online Library][, 2019, Expression of exosomal microRNAs during chondrogenic differentiation of human bone mesenchymal stem cells - Sun - 2019 - Journal of Cellular Biochemistry - Wiley Online

Library][Mao, 2018, Exosomal miR-95-5p regulates chondrogenesis and cartilage degradation via histone deacetylase 2/8]. These findings suggest that the active molecules in exosomes may be an important mechanism underlying their ability to promote chondrogenesis of HUCMSCs. Thus, to a great extent, our results explain the research finding that the co-culture of chondrocytes induces chondrogenesis of mesenchymal stem cells[29,30], which might be due to the stimulation of chondrocyte-secreted exosomes. At present, the exact role of C-EXOs in cartilage repair remains unclear, and we suspect that microRNAs or proteins related to autophagy may play a key role. The contents of C-EXOs are complex, and hence future studies may be needed to analyse further the components and mechanisms involved in cartilage repair for these exosomes. Interestingly, exosomes derived from osteoblast can promote osteogenic differentiation of stem cells in an adipogenic medium environment[16]. These results combined with our findings further support the biological theory that exosomes retain the original biological activities of homologous cells.

Our research also revealed that C-EXOs enhance *Sox9* and *Col2a1* expression, particularly in the late stage of chondrogenic differentiation. Moreover, the upregulated levels of these genes were comparable with TGF-β upregulation. It is worth noting that the expression of Col10, a hypertrophic cartilage-related marker, was upregulated in the TGF-β group. These findings indicated that although TGF-β could promote HUCMSC differentiation into chondrocytes, it was prone to inducing hypertrophic differentiation. This result is in accord with the results of others who reported that TGF-β as a main transforming growth factor causes cartilage hypertrophy during the process of inducing cartilage differentiation[5].

Interestingly, we found that compared with TGF-β, C-EXOs had a superior effect in chondrogenic specificity, as evidenced by remarkably downregulated expression of Col1a (a fibrocartilage marker) and Col10 (a hypertrophic cartilage marker), indicating that C-EXOs can better prevent fibrogenic and hypertrophic differentiation by maintaining the chondrocyte phenotype. This notion of chondrogenesis is further supported by the observations that C-EXO administration accelerated the healing process of cartilage defects and maintained the characteristics of hyaline cartilage, as evidenced by histological findings and macroscopic appearance, which displayed more effective cartilage repair than TGF-β did in a rabbit cartilage defect model. Therefore, C-EXOs possess a robust ability to repair cartilage and cause less hypertrophy, which bypasses the shortcomings of TGF-β.

In our studies, we also observed that the chondrogenic differentiation of HUCMSCs mediated by C-EXOs was accompanied by the activation of autophagy, suggesting that autophagy is probably an essential process during chondrogenic differentiation mediated by C-EXOs. Direct interaction of autophagy and maintenance of chondrocytes has been demonstrated in other studies where autophagy protects chondrocytes from glucocorticoid-induced apoptosis[31,32][Liu, 2014, Autophagy in human articular chondrocytes is cytoprotective following glucocorticoid stimulation], confirming the boosting effect of autophagy on the survival biosynthetic function of chondrocytes. Interestingly, other researchers have shown that autophagy regulates the formation of articular cartilage vesicles in primary articular chondrocytes[33], indicating that there may be mutual regulation between exosomes and autophagy.

Notably, our studies showed no evidence of cell death during the induction of autophagy within the periods in which C-EXOs induced chondrogenic differentiation of HUCMSCs. Besides, we found that C-EXOs could also significantly stimulate HUCMSC migration and proliferation, probably by modulating the cell cycle, although the underlying mechanism needs further clarification. Further studies are required to evaluate the possible use of C-EXOs to stimulate autophagy during chondrogenic differentiation of HUCMSCs and as a therapeutic agent in cartilage defect repair.

Conclusion

In summary, this study characterised C-EXOs from the perspective of cartilage differentiation in HUCMSCs. Our results demonstrate for the first time that human C-EXOs strongly promote differentiation of HUCMSCs into chondrocytes and significantly activate autophagy during the process. These studies shed new light on the development of potential C-EXO therapies that exploit chondrogenesis inductive capabilities.

Materials And Methods

Isolation and culture of HUCMSCs

The sampling scheme of human umbilical cord tissue was approved by the Institutional Review Board of The First Affiliated Hospital of Guangxi Medical University. Signed informed consent was obtained from all participants for this study. The isolation of HUCMSCs from the Wharton's jelly of the umbilical cords was described previously[34] with minor modifications. In brief, umbilical cords were obtained from full-term delivery patients by caesarean section at The First Affiliated Hospital of Guangxi Medical University. The Wharton's jelly was isolated and cut into 1-2-mm^3 pieces, then the growth medium was added and cultured at 37°C in a 5% CO2 humidified incubator. The growth medium was composed of high-glucose Dulbecco's modified Eagle's medium (DMEM; Gibco, USA) and 10% foetal bovine serum (FBS; Gibco, USA) was refreshed every 3 days. After the first subculture, the cells were passaged at a ratio of 1:5 when they reached near 90% confluence. All HUCMSCs undergoing further analysis were used at passages 3-5 in this study.

The osteogenic, adipogenic and chondrogenic differentiation capacity of isolated

HUMSCs were assessed using Osteogenic-Differentiation Medium, Adipogenic-Differentiation Medium, and Complete Chondrogenic Medium (Cyagen Biosciences, Santa Clara, CA, USA). At the end of the incubation period, the differentiation of HUCMSCs was detected by three kinds of staining. Alizarin red solution (Solarbio, Beijing, China), oil red-O staining (Solarbio, Beijing, China), and alcian blue staining (Solarbio, Beijing, China) were used to detect osteogenic differentiation, lipogenic differentiation, and chondrogenic differentiation according to manufacturer's instructions, respectively.

Isolation and culture of mature chondrocytes

Primary chondrocytes were harvested from patients (n=13, average age: 10.8 months, range 6-15 months, male: 7, female: 6) who underwent polydactyly surgery at The First Affiliated Hospital of Guangxi Medical University. Cartilage tissues were obtained from knuckle cartilage and minced into pieces. And then, the cartilage pieces were digested using a 2 mg/mL collagenase type II solution (Sigma, USA) at 37°C for 3 hours after treatment with 0.25% trypsin (Solarbio, Beijing, China) for 30 minutes as described previously[6]. Chondrocytes were cultivated in DMEM culture medium containing 10% foetal bovine serum (Gibco, USA) and 1% penicillin/streptomycin (Solarbio, Beijing, China) at 37°C in a 5% CO2 humidified incubator. The culture medium was replaced by fresh medium every three days. The chondrocytes were re-plated at a ratio of 1:4 when the cells achieved near 100% confluence. All the chondrocytes at passages 3-4 that remained oval or polygonal in shape were used in our studies.

Extraction and identification of exosomes

Chondrocyte-derived exosomes (C-EXOs) were extracted by differential centrifugation, as described previously, with some minor modifications[35,36]. Briefly, the culture medium was collected after chondrocytes were cultured with serum-free medium for 48 hours, centrifuged at 1,000 x*g* at 4°C for 15 minutes to remove dead cells, and then centrifuged at 10,000 x*g* for 30 minutes to remove cell debris and macroparticles. The supernatant was collected and transferred to ultracentrifuge tubes (Beckman Coulter) and ultra-centrifuged at 100,000 x*g* for 1.5 hours using a Thermo Scientific Sorvall WX UltraSeries Centrifuge with an AT-50 rotor. The pellets were collected and washed with PBS by centrifugation at 100,000 x*g* for 1.5 hours. All centrifugation procedures were carried out at 4°C. The purified C-EXOs were resuspended in PBS and stored at -80°C. The C-EXOs were identified by transmission electron microscopy (TEM, H-800, Hitachi, Tokyo, Japan) and a Flow Nano Analyzer (NanoFCM, Xiamen Fuliu Biological Technology Co., China).

Cellular uptake of exosomes

Chondrocyte-derived exosomes (C-EXOs) were first labelled with FITC-CD9 according to the manufacturer's instructions (BD Biosciences, USA). Briefly, 200 μL of the cell-labelling solution was added to 500 μL of an exosome suspension (1.77E + 10 Particles/mL) and incubated at 37°C for 30 minutes. Subsequently, the mixture was washed by PBS twice to remove the free dye, and then the sediment was suspended with 500 μL of PBS. The HUCMSCs were incubated with labelled C-EXOs at 37°C for 12 hours. The HUCMSCs were then fixed with 4% paraformaldehyde at room temperature for 20 minutes after washing with PBS. Next, cells were dyed with phalloidin and DAPI. Confocal images were sequentially acquired by confocal microscopy (TCS SP8, Leica, Germany).

Cell proliferation assay

Cell counting kit-8 (CCK8, Beyotime, Biotechnology, Haimen, China) analysis was used to measure the proliferation of cells. The HUCMSCs were cultured in a 96-well plate. After the cells reached 70%-80% confluence, the culture medium was substituted with 90 μL of a fresh medium comprising various concentrations of C-EXOs and cultured for 24 hours. After that, 10 μL of CCK-8 solution was added to each well, and the optical density (OD) of the culture medium was measured at 450 nm using a microplate reader (Thermo Scientific, USA) after incubation at 37°C for 4 hours following a previously reported study[37].

Cell viability assay

A live/dead cell viability assay was used to measure the viability of HUCMSCs. According to the manufacturer's instructions (Invitrogen, Carlsbad, CA, USA), the staining solution was prepared as 0.5% calcein–acetoxymethyl (calcein-AM) and 2% propidium iodide (PI) in PBS. Then, the treated or untreated HUCMSCs were washed three times with PBS and stained with the staining solution at 37°C for 5 minutes in the dark. Images were captured by the inverted fluorescence microscope (BX53, Olympus, Tokyo, Japan).

Migration assay

The migration of C-EXO-treated HUCMSCs was evaluated using scratch wound assay. HUCMSCs were plated in a 12-well plate (2×10^5 cells/well, three replicates per group) and cultured in a 37°C humidified incubator with 5% CO_2 until cell fusion. The confluent monolayer of cells was scratched using a 10- L micropipette tip and then washed with culture medium three times to remove shed cells. After that, the HUCMSCs were cultured in a serum-free medium contained C-EXOs, TGF-β, or control medium. The images were obtained at the same position at 0 hours, 6 hours, and 12 hours post-wounding. Scratched areas were investigated via Image-J software (National Institutes of Health, Bethesda, MD, USA).

Flow cytometry

Cells were harvested and centrifuged at 1,200 rpm for 5 minutes, and then the pellet was resuspended by adding 50 μL of binding buffer. Followed by the dyes (FITC Annexin V Apoptosis Detection Kit, BD Biosciences) was added in each group and incubated for 15 minutes at room temperature under the dark environment. Then the samples were treated with 200 μL of binding buffer and analysed by flow

cytometry (BD AccuriTMC6 PLUS, BD Biosciences). For C-EXO detection, fluorescently labelled antibody: human CD9 FITC (2 μL, BD Pharmingen™, Catalog No.555371), human CD63 FITC (2 μL, BD Pharmingen™, Catalog No.550759) were added into 50 μL of C-EXOs. After incubation at 37°C for 30 minutes, labelled C-EXOs were washed twice, and then the particles were resuspended in PBS and tested using a Flow Nano Analyzer (NanoFCM, Xiamen Fuliu Biological Technology Co., China).

Autophagy detection

The observation of autophagy was conducted by double-labelled mRFP-GFP-LC3 adenovirus (Shanghai Genechem Co., China) transfection. First, the HUCMSCs were cultured for two days, and then mRFP-GFP-LC3 lentivirus was introduced into HUCMSCs according to the manufacturer's protocol. After that, these cells were treated with PBS, C-EXOs, and TGF-β, respectively, for 48 hours. The formation of autolysosomes was detected and analysed using laser confocal microscopy (TCS SP8, Leica, Germany). Autophagic bodies are represented by yellow spots and autophagic lysosomes by red spots. In addition, cells from different groups were sectioned, and autophagosomes were observed using transmission electron microscopy (TEM, H-800, Hitachi, Tokyo, Japan).

Real-time polymerase chain reactions

Total RNA was extracted from each group of cells using a total RNA isolation kit (Tiangen Biotechnology, Beijing, China) according to the manufacturer's protocol. The quantity and purity of RNA were determined using Nanodrop (Thermo Scientific, USA). One thousand ng of total RNA samples were used to synthesise complementary DNA using a reverse transcription kit (Fermentas, Waltham, MA). Real-time polymerase chain reaction (PCR) was conducted using FastStart Universal SYBR Green Master Mix (Roche Company, Basel, Switzerland) and pre-designed primers for 45 cycles of 15 seconds at 95°C and 1 minute at 60°C as reported previously[38][Chen, 2019, Cartilage-targeting and dual MMP-13/pH responsive theranostic nanoprobes for osteoarthritis imaging and precision therapy][Chen, 2019, Cartilage-targeting and dual MMP-13/pH responsive theranostic nanoprobes for osteoarthritis imaging and precision therapy][Chen, 2019, Cartilage-targeting and dual MMP-13/pH responsive theranostic nanoprobes for osteoarthritis imaging and precision therapy][Chen, 2019, Cartilage-targeting and dual MMP-13/pH responsive theranostic nanoprobes for osteoarthritis imaging and precision therapy][Chen, 2019, Cartilage-targeting and dual MMP-13/pH responsive theranostic nanoprobes for osteoarthritis imaging and precision therapy][Chen, 2019, Cartilage-targeting and dual MMP-13/pH responsive theranostic nanoprobes for osteoarthritis imaging and precision therapy][Chen, 2019, Cartilage-targeting and dual MMP-13/pH responsive theranostic nanoprobes for osteoarthritis imaging and precision therapy][Chen, 2019, Cartilage-targeting and dual MMP-13/pH responsive theranostic nanoprobes for osteoarthritis imaging and precision therapy]. The primer sequences of the genes are listed in Table 1. The expression level of each gene was normalised using glyceraldehyde -3- phosphate dehydrogenase (GAPDH). Each

experiment was repeated three times. The target gene relative expression was calculated using the comparative method $2^{-\Delta}$Ct.

Western blot analysis

The western blot analysis was performed as previously described[39]. Briefly, collected cells were washed with cold PBS and lysed in lysis RIPA buffer containing PMSF (1 mM phenylmethylsulfonyl fluoride). The extracted protein concentration was determined using a BCA protein assay kit (Beyotime, China). Furthermore, each sample with an equal amount of protein (70 μg) was added and separated on 10% SDS-polyacrylamide gel and then transferred to polyvinylidene fluoride membranes. Next, the membranes were incubated with an appropriate concentration of primary antibodies, which are as follows: CD63(1:1,000, Abcam, Catalog No. ab134045), CD9(1:2,000, Abcam, Catalog No. ab92726), TSG101(1:2,000, Abcam, Catalog No. ab125011), CALNEXIN(1:1,000, Abcam, Catalog No. ab22595), SOX9 (1:1,000, CST, Catalog No. 82630), COL2A (1:1,000, Abcam, Catalog No. ab185430), ACAN (1:100, Abcam, Catalog No. ab3778), COL1A (1:1,000, Abcam, Catalog No. ab88147), COL10 (1:300, Abcam, Catalog No. ab58632), Beclin-1 (1:2,000, Abcam, Catalog No. ab207612), ATG7 (1:1,000, Cell Signaling Technology, Catalog No. 2631), P62 (1:1,000, Cell Signaling Technology, Catalog No. 5114), LC3-B (1:2,000, Abcam, Catalog No. ab18709) and GAPDH (1:5,000, Abcam, Catalog No. ab8245). After washing with TBST at 37°C, the membranes were incubated with a secondary antibody (1:15,000, LI-COR, USA). Images were acquired with the Odyssey infrared imaging system (LI-COR Biosciences, Lincoln, NE, USA).

Establishment of animal models

All animal experiments included in this study were approved by The Animal Research Committee of the Guangxi Medical University. The surgical procedure for the rabbit model was performed as previously described[40]. Briefly, clinically healthy New Zealand white rabbits (either sex, 6-months-old, weighing 1-2 kg) were selected randomly for the study. General anaesthesia was administered as 2% pentobarbital sodium through the auricular vein, and the knee joint of the rabbit was exposed through the lateral parapatellar approach. A cartilaginous defect with a diameter of 4.0 mm and a depth of 3.0 mm was made in the medial side of each patella groove using a hand drill. Then, each animal received a local fill with masses of HUCMSCs (2×10^6) in the defect area. The defects were treated as follows: (1) HUCMSCs, which were cultured with complete medium for 14 days (negative control group, n=30 knees); (2) C-EXO-treated HUCMSCs: HUCMSCs were cultured with complete medium including C-EXOs for 14 days, (C-EXO group, n=30 knees); (3) TGF-β-treated HUCMSCs: HUCMSCs were cultured in chondrocyte-inducing medium with TGF-β for 14 days, which served as a positive control. (TGF-β group, n=30 knees). Penicillin was administered for 3 days post-surgery. Euthanasia was performed with an overdose of pentobarbital sodium administered by intravenous (I.V.) injection at 4 or 12 weeks after surgery. The treated condyles

were harvested for further analysis. The International Cartilage Repair Society (ICRS) scoring system was applied to assess the gross morphological phenotype of the cartilage defect repair in rabbit models[41].

Histological examination

The osteochondral blocks containing repaired tissue were harvested, and specimens were decalcified with 14% ethylenediaminetetraacetic acid (EDTA) solution for six to eight weeks after fixation with 10% neutral buffered formalin. The tissue samples were embedded in paraffin and serially sectioned conventionally. The sections were stained with haematoxylin and eosin (H&E), safranin-O/fast green (Solarbio, Beijing, China) and immunohistochemical collagen type II stain (1:200, Bioss, Catalog No. bs-0709R) according to the standard protocols, then were observed using light microscopy (Olympus BX53, Tokyo, Japan). The results were scored by three qualified examiners who were blinded to the outcome of the cases according to the ICRS Visual Histological Assessment Scale [42].

Immunofluorescence analysis

Immunofluorescence examination was performed as previously described[39]. For cell immunofluorescence preparation, planted cells were fixed by 4% paraformaldehyde, successively treated with 3% H_2O_2 for 10 minutes and blocked with goat serum at room temperature for 10 minutes. The primary antibody COL2A was used to detect changes in chondrogenic differentiation. Samples were incubated with anti-COL2A antibody (1:200, Boster, China) at 37°C for three to four hours, followed by incubation with the secondary antibody (anti-rabbit antibody, 1:50, Boster, China) at 37°C for 45 minutes, the nuclei were counterstained with 4', 6-diamidino-2-phenylindole (DAPI; Boster) for 5 minutes. Images were obtained sequentially using a fluorescence microscope (Olympus BX53, Tokyo, Japan).

Statistical analysis

All data collected in this study are analysed in SPSS (SPSS v22.0; IBM, Armonk, NY). The statistical significance between the two groups was evaluated using a one-way analysis of variance with a t-test. A $P < 0.05$ was considered a statistically significant difference.

Declarations

Competing interests

No potential conflicts of interest were disclosed.

Acknowledgments

This study was financially supported by the National Key R&D Program of China (Grant No. 2018YFC1105900), the Guangxi Key Research and Development Plan (Grant No. GuikeAD17129012), the Guangxi Natural Science Foundation Program (Grant No. 2019GXNSFAA185004), the Distinguished Young Scholars Program of Guangxi Medical University, the Guangxi Collaborative Innovation Centre of Biomedicine (Grant No. GCICB-IE-2018004), the Innovation Project of Guangxi Graduate Education (Grant No. YCSW2019109).

Author contributions

K.M. and B.Z. conceived the research, designed and implemented the experiments, collected and analysed data, wrote the manuscript, and contributed equally in this investigation. L.Y.: guided the stem cell experiments, and provided final approval of the manuscript; L.Z.: guided the design and implementation of the experiments, revised drafts of the manuscript, and granted final approval of the manuscript; J.Z.: directed the experiment, and provided final approval of the manuscript; Z.W., P.C, M.H., D.Y. and G.Y.: implemented the experiments and collected data.

Data availability statement

The data supporting the findings of this study are available from the corresponding author upon reasonable request.

References

1 Demoor, M. *et al.* Cartilage tissue engineering: Molecular control of chondrocyte differentiation for proper cartilage matrix reconstruction. *Biochimica et Biophysica Acta (BBA) - General Subjects* **1840**, 2414-2440, doi:10.1016/j.bbagen.2014.02.030 (2014).

2 Mizuno, M. *et al.* Brief Report: Reconstruction of Joint Hyaline Cartilage by Autologous Progenitor Cells Derived from Ear Elastic Cartilage. *Stem Cells* **32**, 816-821, doi:10.1002/stem.1529 (2014).

3 Jayasuriya, C. T., Chen, Y., Liu, W. & Chen, Q. The influence of tissue microenvironment on stem cell–based cartilage repair. *Ann N Y Acad Sci* **1383**, 21-33, doi:10.1111/nyas.13170 (2016).

4 Wang, W.-G., Lou, S.-Q., Ju, X.-D., Xia, K. & Xia, J.-H. In vitro chondrogenesis of human bone marrow-derived mesenchymal progenitor cells in monolayer culture: activation by transfection with TGF-β2. *Tissue and Cell* **35**, 69-77, doi:10.1016/s0040-8166(02)00106-4 (2003).

5 Deng, Y. *et al.* Engineering hyaline cartilage from mesenchymal stem cells with low hypertrophy potential via modulation of culture conditions and Wnt/beta-catenin pathway. *Biomaterials* **192**, 569-578, doi:10.1016/j.biomaterials.2018.11.036 (2019).

6 Danisovic, L., Varga, I. & Polak, S. Growth factors and chondrogenic differentiation of mesenchymal stem cells. *Tissue Cell* **44**, 69-73, doi:10.1016/j.tice.2011.11.005 (2012).

7 Zhan, X. *et al.* Comparative profiling of chondrogenic differentiation of mesenchymal stem cells (MSCs) driven by two different growth factors. *Cell Biochem Funct* **37**, 359-367, doi:10.1002/cbf.3404 (2019).

8 Valadi, H. *et al.* Exosome-mediated transfer of mRNAs and microRNAs is a novel mechanism of genetic exchange between cells. *Nat Cell Biol* **9**, 654-659, doi:10.1038/ncb1596 (2007).

9 Xu, R., Greening, D. W., Zhu, H. J., Takahashi, N. & Simpson, R. J. Extracellular vesicle isolation and characterization: toward clinical application. *J Clin Invest* **126**, 1152-1162, doi:10.1172/JCI81129 (2016).

10 Lai, R. C., Yeo, R. W. & Lim, S. K. Mesenchymal stem cell exosomes. *Semin Cell Dev Biol* **40**, 82-88, doi:10.1016/j.semcdb.2015.03.001 (2015).

11 S, Z. *et al.* MSC exosomes mediate cartilage repair by enhancing proliferation, attenuating apoptosis and modulating immune reactivity. *Biomaterials* **156**, 16-27 (2018).

12 Raposo, G. & Stoorvogel, W. Extracellular vesicles: exosomes, microvesicles, and friends. *J Cell Biol* **200**, 373-383, doi:10.1083/jcb.201211138 (2013).

13 Robbins, P. D. & Morelli, A. E. Regulation of immune responses by extracellular vesicles. *Nat Rev Immunol* **14**, 195-208, doi:10.1038/nri3622 (2014).

14 Riazifar, M., Pone, E. J., Lotvall, J. & Zhao, W. Stem Cell Extracellular Vesicles: Extended Messages of Regeneration. *Annu Rev Pharmacol Toxicol* **57**, 125-154, doi:10.1146/annurev-pharmtox-061616-030146 (2017).

15 Zhao, T. *et al.* Emerging Role of Mesenchymal Stem Cell-derived Exosomes in Regenerative Medicine. *Curr Stem Cell Res Ther* **14**, 482-494, doi:10.2174/1574888X14666190228103230 (2019).

16 Narayanan, K. *et al.* Lineage-specific exosomes could override extracellular matrix mediated human mesenchymal stem cell differentiation. *Biomaterials* **182**, 312-322, doi:10.1016/j.biomaterials.2018.08.027 (2018).

17 W, J. *et al.* Large-scale generation of cell-derived nanovesicles. *Nanoscale* **6**, 12056-12064 (2014).

18 Chen, Y., Xue, K., Zhang, X., Zheng, Z. & Liu, K. Exosomes derived from mature chondrocytes facilitate subcutaneous stable ectopic chondrogenesis of cartilage progenitor cells. *Stem Cell Research & Therapy* **9**, doi:10.1186/s13287-018-1047-2 (2018).

19 Hoffmann, A., Floerkemeier, T., Melzer, C. & Hass, R. Comparison of in vitro-cultivation of human mesenchymal stroma/stem cells derived from bone marrow and umbilical cord. *J Tissue Eng Regen Med* **11**, 2565-2581, doi:10.1002/term.2153 (2017).

20 Yin, S., Ji, C., Wu, P., Jin, C. & Qian, H. Human umbilical cord mesenchymal stem cells and exosomes: bioactive ways of tissue injury repair. *Am J Transl Res* **11**, 1230-1240 (2019).

21 Ding, D. C., Chang, Y. H., Shyu, W. C. & Lin, S. Z. Human umbilical cord mesenchymal stem cells: a new era for stem cell therapy. *Cell Transplant* **24**, 339-347, doi:10.3727/096368915X686841 (2015).

22 Salemi, S., Yousefi, S., Constantinescu, M. A., Fey, M. F. & Simon, H. U. Autophagy is required for self-renewal and differentiation of adult human stem cells. *Cell Res* **22**, 432-435, doi:10.1038/cr.2011.200 (2012).

23 Wu, X. *et al.* Autophagy regulates Notch degradation and modulates stem cell development and neurogenesis. *Nat Commun* **7**, 10533, doi:10.1038/ncomms10533 (2016).

24 Colao, I. L., Corteling, R., Bracewell, D. & Wall, I. Manufacturing Exosomes: A Promising Therapeutic Platform. *Trends in Molecular Medicine* **24**, 242-256, doi:10.1016/j.molmed.2018.01.006 (2018).

25 Mao, G. *et al.* Exosomes derived from miR-92a-3p-overexpressing human mesenchymal stem cells enhance chondrogenesis and suppress cartilage degradation via targeting WNT5A. *Stem Cell Res Ther* **9**, 247, doi:10.1186/s13287-018-1004-0 (2018).

26 Mao, G. *et al.* in *J Cell Mol Med* Vol. 22 5354-5366 (2018).

27 Expression of exosomal microRNAs during chondrogenic differentiation of human bone mesenchymal stem cells - Sun - 2019 - Journal of Cellular Biochemistry - Wiley Online Library. doi:10.1002/jcb.27289 (2019).

28 Wang, R., Xu, B. & Xu, H. TGF-beta1 promoted chondrocyte proliferation by regulating Sp1 through MSC-exosomes derived miR-135b. *Cell Cycle* **17**, doi:10.1080/15384101.2018.1556063 (2018).

29 X, L. *et al.* In vivo ectopic chondrogenesis of BMSCs directed by mature chondrocytes. *Biomaterials* **31**, 9406-9414 (2010).

30 C, L. *et al.* Kartogenin Enhanced Chondrogenesis in Cocultures of Chondrocytes and Bone Mesenchymal Stem Cells. *Tissue engineering. Part A* **24**, 990-1000 (2018).

31 Liu, N., Wang, W., Zhao, Z., Zhang, T. & Song, Y. Autophagy in human articular chondrocytes is cytoprotective following glucocorticoid stimulation. *Mol Med Rep* **9**, 2166-2172, doi:10.3892/mmr.2014.2102 (2014).

32 Shen, C., Cai, G. Q., Peng, J. P. & Chen, X. D. Autophagy protects chondrocytes from glucocorticoids-induced apoptosis via ROS/Akt/FOXO3 signaling. *Osteoarthritis Cartilage* **23**, 2279-2287, doi:10.1016/j.joca.2015.06.020 (2015).

33 Rosenthal, A. K. *et al.* Autophagy modulates articular cartilage vesicle formation in primary articular chondrocytes. *J Biol Chem* **290**, 13028-13038, doi:10.1074/jbc.M114.630558 (2015).

34 Maldonado, M., Huang, T., Yang, L., Xu, L. & Ma, L. Human umbilical cord Wharton jelly cells promote extra-pancreatic insulin formation and repair of renal damage in STZ-induced diabetic mice. *Cell Commun Signal* **15**, 43, doi:10.1186/s12964-017-0199-5 (2017).

35 Zhu, Y. *et al.* Comparison of exosomes secreted by induced pluripotent stem cell-derived mesenchymal stem cells and synovial membrane-derived mesenchymal stem cells for the treatment of osteoarthritis. *Stem Cell Res Ther* **8**, 64, doi:10.1186/s13287-017-0510-9 (2017).

36 Coumans, F. A. W. *et al.* Methodological Guidelines to Study Extracellular Vesicles. *Circulation Research* **120**, 1632-1648, doi:10.1161/circresaha.117.309417 (2017).

37 Jiang, T. *et al.* In vitro expansion impaired the stemness of early passage mesenchymal stem cells for treatment of cartilage defects. *Cell Death Dis* **8**, e2851, doi:10.1038/cddis.2017.215 (2017).

38 Chen, H. *et al.* Cartilage-targeting and dual MMP-13/pH responsive theranostic nanoprobes for osteoarthritis imaging and precision therapy. *Biomaterials* **225**, 119520, doi:10.1016/j.biomaterials.2019.119520 (2019).

39 Shen, C. *et al.* In vitro culture expansion impairs chondrogenic differentiation and the therapeutic effect of mesenchymal stem cells by regulating the unfolded protein response. *J Biol Eng* **12**, 26, doi:10.1186/s13036-018-0119-2 (2018).

40 Liao, J. *et al.* The fabrication of biomimetic biphasic CAN-PAC hydrogel with a seamless interfacial layer applied in osteochondral defect repair. *Bone Res* **5**, 17018, doi:10.1038/boneres.2017.18 (2017).

41 van den Borne, M. P. *et al.* International Cartilage Repair Society (ICRS) and Oswestry macroscopic cartilage evaluation scores validated for use in Autologous Chondrocyte Implantation (ACI) and microfracture. *Osteoarthritis Cartilage* **15**, 1397-1402, doi:10.1016/j.joca.2007.05.005 (2007).

42 Guo, X. *et al.* Repair of osteochondral defects with biodegradable hydrogel composites encapsulating marrow mesenchymal stem cells in a rabbit model. *Acta Biomater* **6**, 39-47, doi:10.1016/j.actbio.2009.07.041 (2010).

Table

Table 1

Primers for real-time polymerase chain reaction

Gene names	Forward primer	Reverse primer
Col 2a	CCGTGCTCCTGCCGTTTC	CTGAGGCAGTCTTTCACGTCT
Sox-9	AAGCTCTGGAGACTTCTGAACG	CGTTCTTCACCGACTTCCTCC
Acan	CTACACGCTACACCCTCGAC	ACGTCCTCACACCAGGAAAC
Col 10	CGATACCAAATGCCCACAGG	ATGGTCCTCTCTCTCCTGGT
Col 1a	GTTCAGCTTTGTGGACCTCCG	GCAGTTCTTGGTCTCGTCAC
GAPDH	GTCAAGGCTGAGAACGGGAA	AAATGAGCCCCAGCCTTCTC

Note. Col2a, collagen type II; Sox9, SRY-related high mobility group-box gene 9; Acan, aggrecan; Col10, collagen type; Col1a, collagen type I; GAPDH: glyceraldehyde-3-phosphate dehydrogenase.

Figures

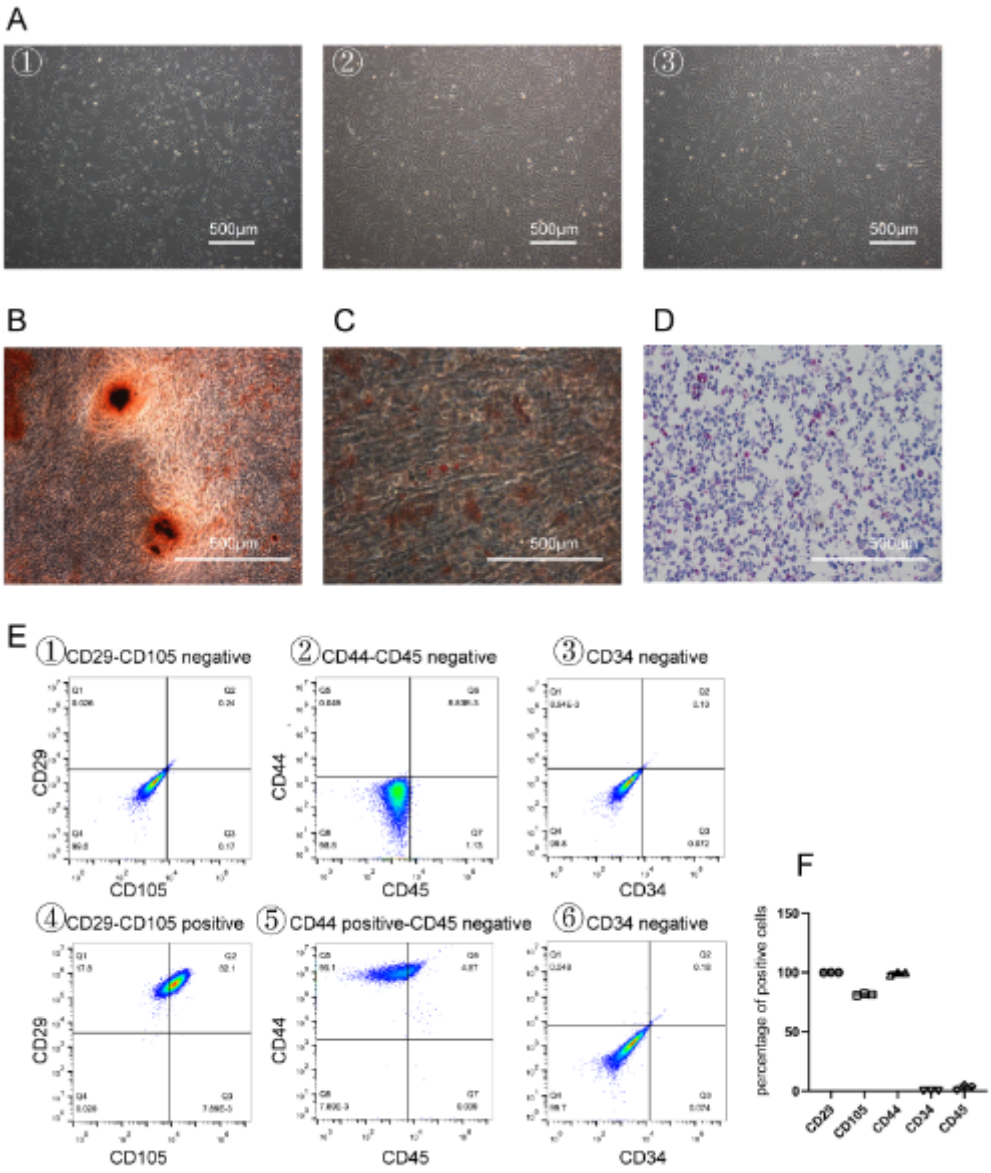

Figure 1

Detection of HUCMSC characteristics. (A) The representative spindle-like morphology of HUCMSCs in passages 3-5 were observed by microscopy. The multipotency of HUCMSCs for osteogenesis, adipogenesis, and chondrogenesis was determined by alizarin red staining (B), oil-red-o staining (C), and haematoxylin-eosin and alcian blue dual-staining (D), respectively. Scale bar = 500 μm. (E) Flow cytometric analysis of mesenchymal-related markers: CD29, CD105, CD44, CD45, CD34. □□□were cells without antibodies as negative controls, and □□□were flow cytometry results after adding a fluorescent antibody. This experiment was independently repeated three times. (F) The rates of each marker-positive cells (n = 3).

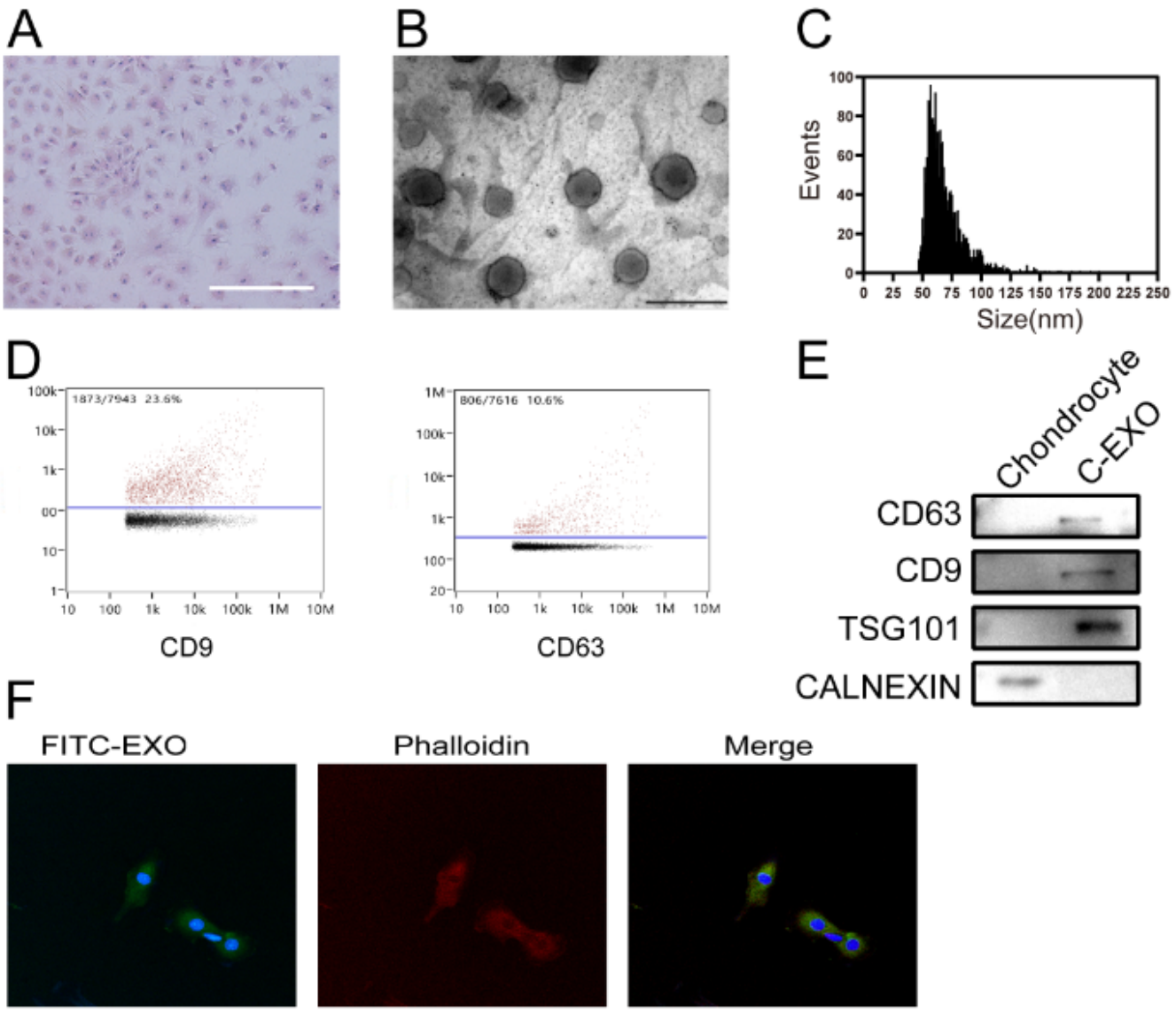

Figure 2

Characterisation of human chondrocyte-derived exosomes (C-EXOs). (A) The morphology of chondrocytes was observed using haematoxylin-eosin staining. Scale bar=500 μm. (B) The morphology of C-EXOs was analysed by transmission electron microscopy. Scale bar=200 nm. (C) The particle size distribution of C-EXOs was measured using a flow nano analyser. (D) The expression of CD9 and CD63 in C-EXOs was measured using a flow nano analyser. (E) Western blotting analysis of the protein levels of CD63, CD9, TSG101, and CALNEXIN in C-EXOs and chondrocytes. (F) The representative immunofluorescence photomicrograph for cellular uptake of FITC-labelled C-EXOs (green) was obtained using confocal microscopy. Scale bar=50 μm.

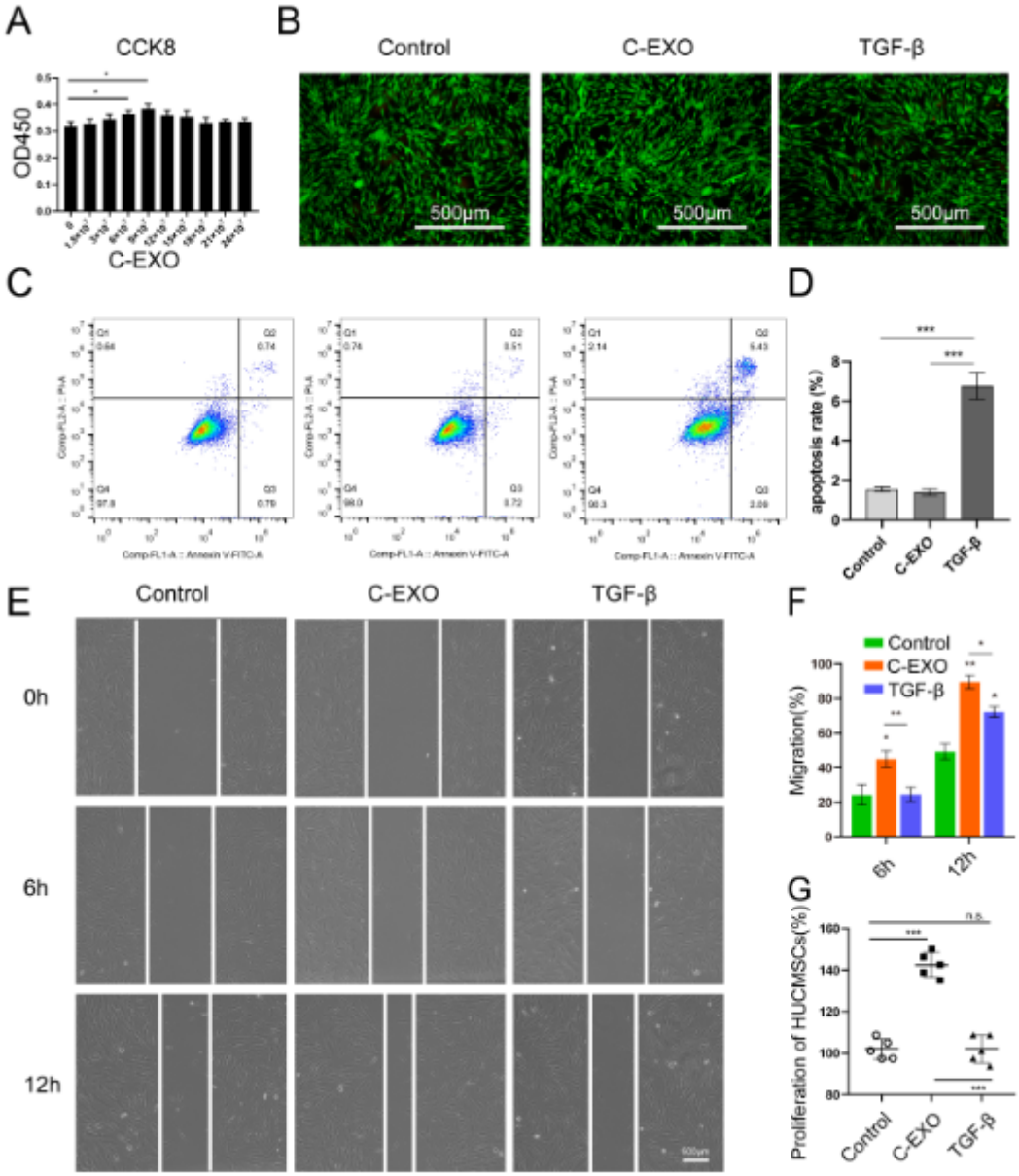

Figure 3

The effects of C-EXOs on migration and proliferation in HUCMSCs. (A) The cytotoxicity of HUCMSCs was detected after treatment with C-EXOs at different doses using the CCK-8 assay. The quantitative data are presented as the means ± standard deviations (SD) of three independent experiments. *p <0.05. (B) Representative images of the live/dead cell staining of HUCMSCs after treatment with PBS, C-EXOs, or TGF-β were obtained by fluorescence microscopy. Scale bar=500 μm. (C) The apoptotic index was determined using flow cytometry analysis. (D) Quantitative estimation of the proportion of apoptotic cells from (C), the quantitative data are presented as the means ± SD of three independent experiments. *p<0.05, **p<0.01. (E) The light microscopic images from the scratch wound assay. Scale bar=500 μm. (F) The quantitative analysis of HUCMSC migration at 6 hours and 12 hours, the quantitative data are presented as means ± SD of three independent experiments. *p <0.05, **p <0.01. (G) The counts of HUCMSCs in different groups at 12 h. n.s., no significant difference, ***p <0.001.

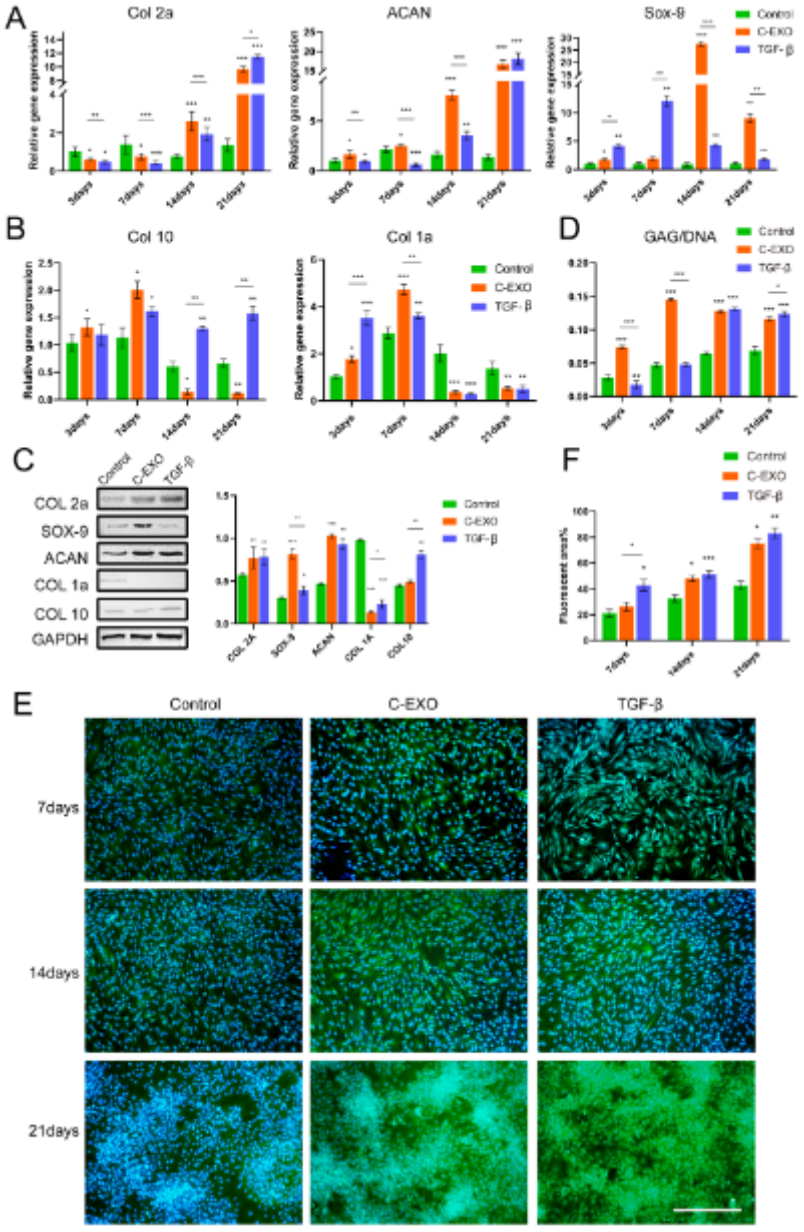

Figure 4

C-EXOs promote the chondrogenic differentiation of HUCMSCs. The expression levels of chondrocyte-specific markers Col2a, ACAN, and Sox9 (A), the hypertrophic cartilage marker Col10, and the fibrocartilage marker Col1a (B) in C-EXO-stimulated HUCMSCs were determined using RT-PCR analysis. These data are presented as the means ± SD of three independent experiments. *p <0.05, **p <0.01, ***p <0.001. (C) The amount of COL2A, SOX9, ACAN, COL1A, and COL10 protein was determined using western blot analysis of HUCMSCs 21 days after treatment with PBS, C-EXOs, or TGF-β. GAPDH was used as a loading control. (D) The quantification of DNA and GAG was performed using biochemical assays, and the ratio of GAG/DNA was calculated. HUCMSCs were cultured with PBS, C-EXOs, or TGF-β for 3, 7, 14, and 21 days. These data are presented as the mean ± SD of three independent experiments. *p <0.05, **p <0.01, ***p <0.001. (E) Immunofluorescence staining for COL2A in HUCMSCs treated with or without

C-EXOs in vitro. Scale bar=500 μm. (F) Quantitative results of immunofluorescence in figure 4E, *p <0.05, **p <0.01, ***p <0.001.

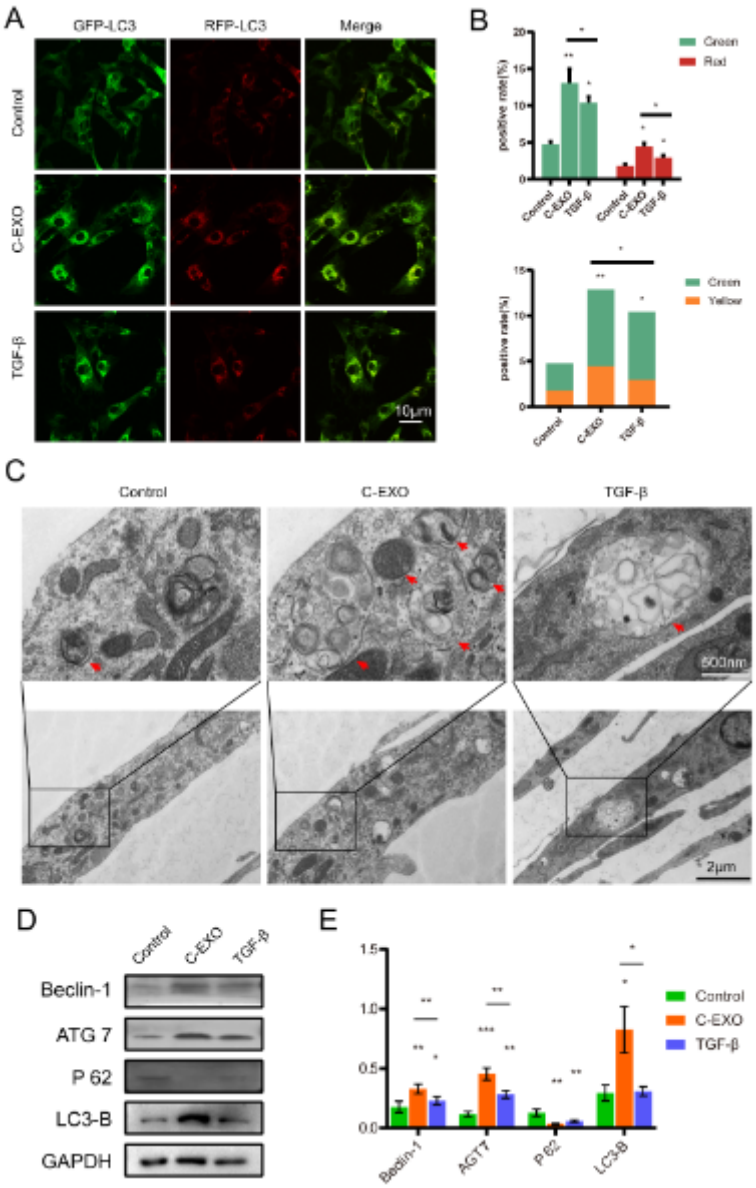

Figure 5

C-EXO treatment induces the activation of autophagy in HUCMSCs. (A) The autophagic flux of mRFP-GFP-LC3-transfected HUCMSCs was revealed using laser confocal microscopy. Autophagosomes are labelled by red and green fluorescence (yellow spots), whereas autophagic lysosomes are labelled by red fluorescence (red spots). (B) The percentage of fluorescence from (A) were quantified and presented as the means ± SD of three independent experiments. *p <0.05, **p <0.01, ***p <0.001. (C) The formation of autophagic vacuoles was observed by transmission electron microscopy. Boxed regions are enlarged and shown in insets. Red arrows indicate autophagic vacuoles. Scale bar=2 μm. (D) HUCMSCs and C-EXOs were incubated for 14 days, and then western blot analysis of autophagy-associated protein levels was performed. (E) Beclin-1, ATG7, P62, and LC3-B protein expressions were quantified and referred to GAPDH, then presented as the mean ± SD for each group. *p <0.05, **p <0.01, ***p <0.001.

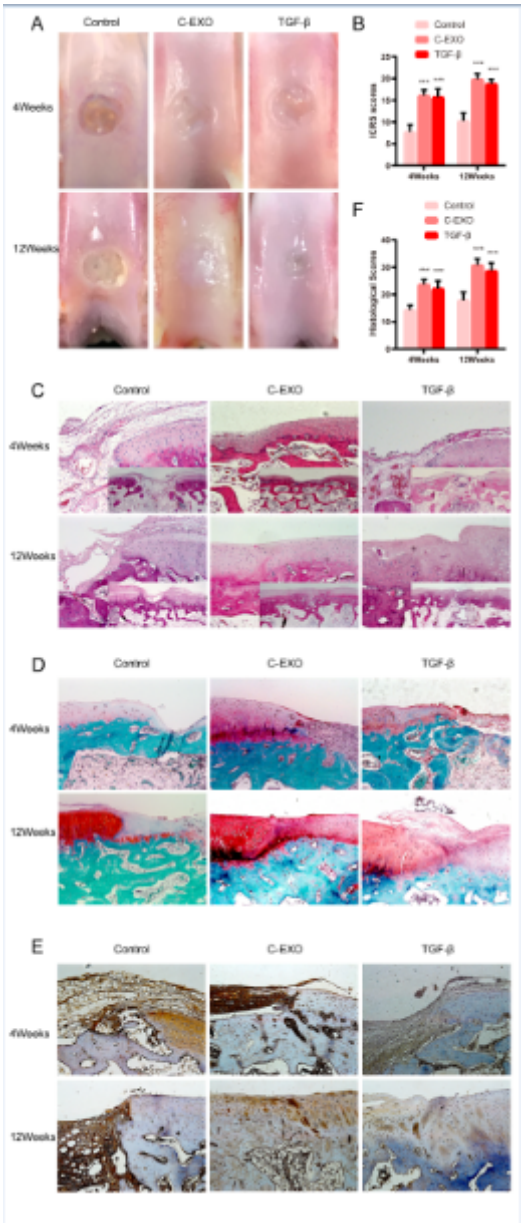

Figure 6

The therapeutic effect of C-EXOs on articular cartilage defects in the rabbit model. (A) Gross morphology of repaired cartilage of the control group, The C-EXO group, and the TGF-β group at 4 weeks and 12 weeks post-surgery. (B) Macroscopic scores of regenerative tissues from the control group, the C-EXO group, and the TGF-β group. n=12. ***p <0.001. (C) H&E staining of repaired cartilage from the control group, the C-EXO group, and the TGF-β group. (D) Safranin O-fast green staining of repaired cartilage from the control group, the C-EXO group, and the TGF-β group. (E) Immunohistochemical staining of collagen type Ⅱ in repaired cartilage from the control group, the C-EXO group, and the TGF-β group. (F) Histological scores of regenerative tissues from each group. n=12. ***p <0.001.

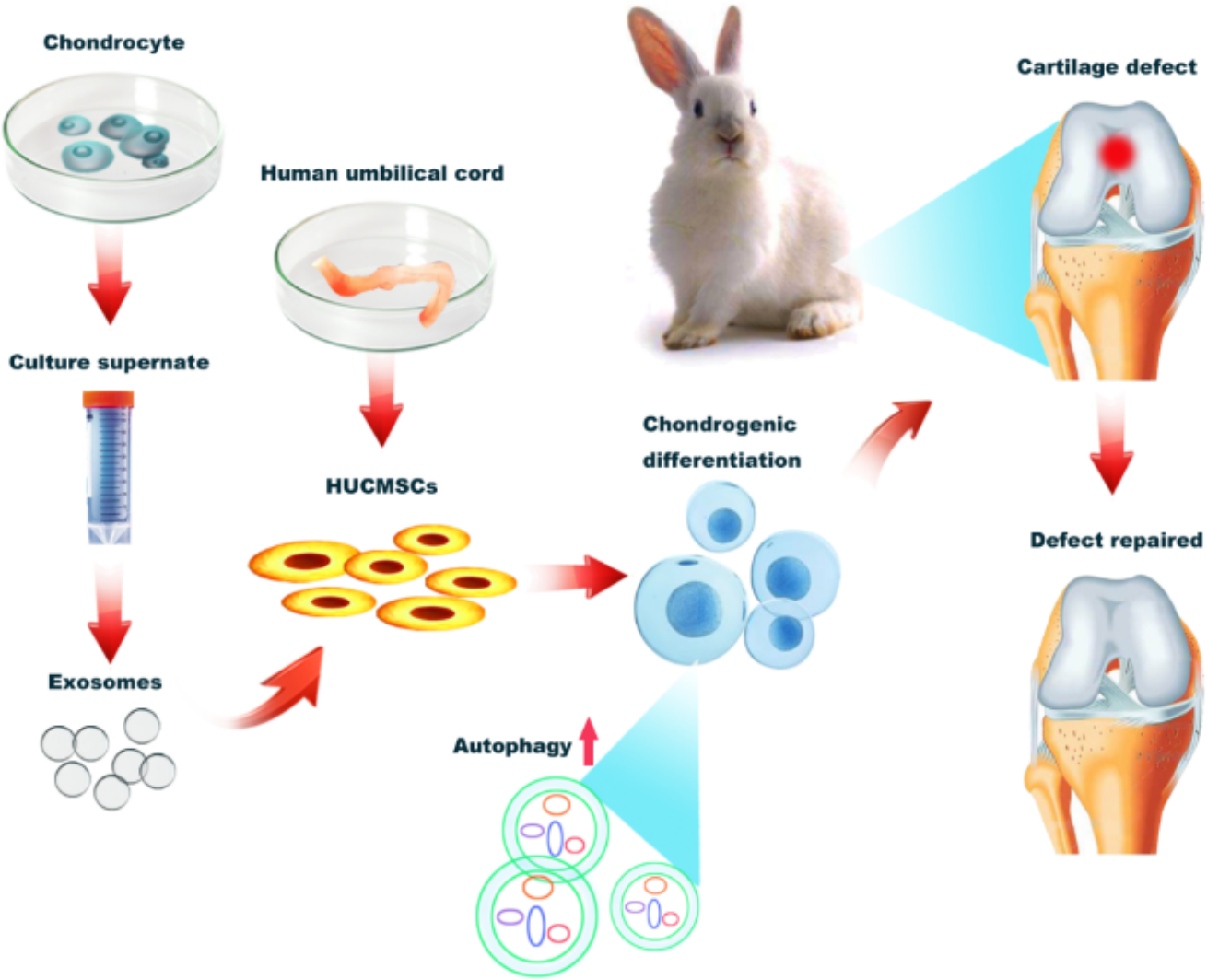

Figure 7

The schematic shows that articular chondrocyte-derived exosomes (C-EXOs) promoted chondrogenic differentiation of human umbilical cord mesenchymal stem cells (HUCMSCs) and enhanced cartilage repair in vivo, meanwhile, autophagy was activated during the induction of HUCMSC differentiation.

Supplementary Files

This is a list of supplementary files associated with this preprint. Click to download.

- FigS12.tif